LRP 538/96 February 1996

THE EFFECT OF PARTIAL POLOIDAL WALL SECTIONS ON THE WALL STABILIZATION OF EXTERNAL KINK MODES

D.J. Ward

To be published in
Physics of Plasmas

THE EFFECT OF PARTIAL POLOIDAL WALL SECTIONS ON THE WALL STABILIZATION OF EXTERNAL KINK MODES

D. J. Ward

Centre de Recherches en Physique des Plasmas, Association Euratom–Confédération Suisse, Ecole Polytechnique Fédérale de Lausanne, 1007 Lausanne, Switzerland

Abstract

An analysis of the effect on the wall stabilization of external kink modes due to toroidally continuous gaps in the resistive wall is performed. The effects both with and without toroidal rotation are studied. For a high-β equilibrium, the mode structure is localized on the outboard side. Therefore, outboard gaps greatly increase the growth rate when there is no rotation. For resistive wall stabilization by toroidal rotation, the presence of gaps has the same effect as moving the wall farther away, i.e., destabilizing for the ideal plasma mode, and stabilizing for the resistive wall mode. The region of stability, in terms of wall position, is reduced in size and moved closer to the plasma. However, complete stabilization becomes possible at considerably reduced rotation frequencies. For a high-β, reverse-shear equilibrium both the resistive wall mode and the ideal plasma mode can be stabilized by close fitting discrete passive plates on the outboard side. The necessary toroidal rotation frequency to stabilize the resistive wall mode using these plates is reduced by a factor of three compared to that for a poloidally continuous and complete wall at the same plasma-wall separation.

PACS numbers: 52.35.Py, 52.30.-q, 52.55.Fa

I. Introduction

The ideal, pressure-driven kink instability in tokamaks imposes a serious limitation on tokamak performance by limiting β, the ratio of plasma-particle pressure to magnetic field pressure ($\beta \equiv 2\mu_0\langle p\rangle/\langle B^2\rangle$, where $\langle\cdots\rangle$ denotes the volume average). Numerical calculations[1] have shown that the normalized beta $\beta_N(\equiv \beta aB/I_p)$ is limited to $\beta_N \approx 3$ by these instabilities. Subsequent numerical studies and many experiments have verified the beta limit, although profile and shape optimization has increased the limit in normalized beta to $\beta_N \approx 4-5$.[2]

The instabilities can be stabilized by the presence of a nearby, perfectly conducting wall. However, in realistic experiments resistive conductors can only slow the instability down to the L/R time-scale of the wall. Some time ago, it was proposed[3] that in a rotating plasma, the resistive wall would act like a perfectly conducting wall for non-axisymmetric stabilities, owing to the fact that the helical eddy currents would rotate faster than the L/R time-scale of the wall and thus not decay. This would therefore stabilize the mode. However, it was later shown,[4] in an analytic calculation using a very simplified model in slab geometry, that a resistive wall with rotation would not stabilize the kink mode, but rather the mode would be fixed with respect to the wall and grow on the resistive time scale.

More recently, numerical calculations[5,6] have shown that both of these simplified theories are partially correct. There are, in fact, two modes that must be stabilized simultaneously. These calculations, which were done for realistic toroidal equilibria with rational surfaces and using a mechanism for dissipation of the sound waves to approximate ion Landau damping, have shown that pressure-driven kink modes could indeed be completely stabilized given sufficient toroidal rotation. The first of these two modes, the ideal "plasma mode," which does not penetrate the wall and rotates very quickly with respect to the wall in the manner suggested by Yoshida and Inoue,[3] is stabilized by the resistive wall acting like a

perfect conductor. Therefore, the mode is stabilized when the plasma-wall separation is less than that for the marginal value of MHD stability of the ideal kink mode with an ideal wall.

The second, the "resistive-wall mode," corresponding to the mode which was not stabilized in the model of Ref. 4, has a very small real frequency with respect to the wall (it is nearly locked to the wall). It was shown,[5–7] that this mode can be stabilized given sufficient rotation, dissipation of sound waves in the plasma, and if the wall position is farther than some minimum plasma-wall separation. This threshold wall position moves closer to the plasma with increasing rotation speed, and a significant region of stability in terms of wall position, which lies between the marginal wall position for the plasma mode and the resistive wall mode, is opened given sufficient rotation.

Considerable experimental evidence[8–13] now exists that demonstrates that toroidal rotation does stabilize pressure-driven kink modes in tokamaks and leads to experimental beta-values significantly above the beta limit for such modes. Analysis of experimental shots and comparison to the new resistive wall mode theories[11,12] indicate a good agreement between experiment and theory. There has been considerable additional theoretical work[7,14,15] which substantiates and expands upon the early calculations.

In this paper, the effect of toroidally continuous gaps in the wall on the stability of resistive wall modes is considered. We will look at both the effect of these gaps on the instability (its growth rate and structure) without rotation, and on the stabilization of resistive wall modes by toroidal rotation. The calculations are performed using a modified version[6] of the NOVA-W code.[16,17]

II. Partial Walls With No Rotation

The effect of toroidally continuous gaps in the resistive wall on the passive growth rates with no rotation will be considered first. Calculations were performed to find the

growth rates of an equilibrium surrounded by a resistive wall with gaps at the inboard and outboard midplane. Figure 1 shows the geometry of the conformal resistive wall with the poloidal gaps. In the following figures, positive values of θ will represent the angular extent of a toroidally continuous gap centered at the inboard midplane, while negative values of θ represent gaps centered at the outboard midplane. (Here, θ measures the angular half-width of the gap, which is symmetric about the midplane.)

Because of the importance of wall stabilization for advanced tokamak equilibria[18] (with reverse-shear, high-β, high bootstrap fraction) we will focus on such equilibria. The primary equilibrium considered here is a reverse-shear equilibrium that was used for calculations presented in Ref. 6. This particular equilibrium is identical to that in in Fig. 9 of Ref. 6 at $\beta^* = 5.2\%$ (β^* is the rms value of β, i.e., $\beta^* \equiv 2\mu_0\langle p^2\rangle^{1/2}/\langle B^2\rangle$). This equilibrium is very similar to the equilibria described in Ref. 18. It has $q_0 = 2.5, q_{min} \approx 2.2, q_s = 4.1$, very high pressure, and a bootstrap fraction of nearly unity with the bootstrap current well aligned with the total plasma current. It is stable everywhere to ballooning modes and has good stability properties with respect to various microinstabilities,[18] but is unstable to the low-n, external, pressure driven kink. In the absence of a conducting wall, the limit in β^* is 2.49%.

In Fig. 2 the growth rate normalized to the wall time, $\gamma\tau_w$ (here, $\tau_w = \mu_0\delta d/\eta$) is plotted with respect to the magnitude of the gaps on the inboard and outboard sides. We see that the growth rate is hardly effected when a gap is introduced on the inboard side for this high-β reverse-shear case. In fact, the entire inboard wall can be removed without noticeably increasing the growth rate. It is only when the value of θ is increased so that the gap extends to the upper and lower parts of the wall and reaches the outboard side that the growth rate begins to increase significantly.

By contrast, even a small gap on the outboard midplane causes the growth rate to increase rapidly. In fact, a gap of half-width $|\theta| = 0.0281\pi$ (5.1°) on the outboard midplane results in a growth rate ($\gamma\tau_w = 10$) as high as removing the entire inboard wall to $\theta =$

$\pm 0.245\pi$ (44.2°). Clearly the stabilizing eddy currents in the wall and the overall mode structure must be concentrated near the outboard midplane. This is not surprising because of the ballooning nature of the high-β, pressure-driven kink.

Figure 3 shows the magnitude of the induced eddy currents in the wall the poloidal plane at toroidal angle $\phi = 0$ for this this equilibrium in terms of the normalized poloidal angle s. Here, $s = 0$ (and $s = 1$) refers to the outboard midplane, and $s = 0.5$ denotes the inboard midplane. The number of peaks reflect the dominant $m = 5$ harmonic at the edge, but the mixing of the other harmonics with large magnitude results in a concentration of the induced currents at the outboard side. It is clear that removing a section of the wall on the outboard side has a much greater effect than removing part of the inboard side.

For comparison let us consider a case using an equilibrium which is a circular, zero-pressure equilibrium with $q_0 = 1.2$, $q_s = 1.9$ and a monotonic q-profile. In Fig. 4 the growth rate is plotted with respect to the angular extent of the gap on the inboard or outboard side in the same way as Fig. 2. Clearly this case is much more symmetric than in the high-β case. There is only a slight increase in growth rate for an outboard gap over that for an inboard gap with the same magnitude, which can be attributed to the finite aspect ratio ($R/a = 3$) of this equilibrium.

In Fig. 5 we see the induced wall currents for this equilibrium with a complete resistive wall. Here, the number of peaks reflects the very dominant $m = 2$ harmonic, and the other harmonics contribute very little, so that the induced wall currents are a nearly symmetric $m = 2$ pattern.

A. Deformations of the eigenfunction

It has been shown[19] for $n = 0$ modes that localized poloidal sections of passive conductor can alter the eigenfunction and thus the eddy current pattern so that the stabilizing effect of the eddy currents is reduced. When there is only a pair of conducting plates (as opposed

to a continuous resistive wall) the harmonics of the eigenfunction are modified so as to reduce the stabilizing eddy currents in those plates compared to the eigenfunction for the case of a complete, continuous resistive wall.

Figure 6 shows how the eigenfunction of the instability is affected by the removal of sections of the resistive wall. Plotted are the values of the $m = 2, 3, 4$ harmonics (at the plasma edge) vs. the angular magnitude of poloidal gaps on the inboard and outboard sides. Also plotted is the normalized growth rate (here, $\gamma\tau_w/20$ is plotted to match the scale of the harmonics of the eigenfunction). The variation of the harmonics are greatest where the increase of the growth rate is the highest. When the magnitude of the gap is increased on the outboard side, there is a decrease in the magnitude of the $m = 2, 3, 4$ harmonics, and is steepest for the $m = 3$ harmonic. The changes in the eigenfunction due to removing the inboard wall (positive θ) are in the opposite sense, and are not as sharp.

Figure 7 shows how the changes with the eigenfunction caused by the modifications of the resistive wall alter the induced eddy currents in such a way that their stabilizing effect is reduced. Plotted in Fig. 7 are the magnitudes of the induced currents with a complete resistive wall (solid line—as in Fig. 3) and that for the case with a gap of magnitude $\Delta\theta = 0.209\pi$ (38°) in the outboard side (dashed line). Of course, the eddy currents in the gap are zero, and we see that the region with the large eddy currents on the outboard side is pushed further towards the outboard side with respect to the case with a complete resistive wall. The modifications of the eigenfunction effectively push the large eddy currents "into the gap." Increasing the gap size also increases the shift of these induced currents toward the gap, as well as decreasing the width of the eddy current peaks. These modifications to the eigenfunction increase the growth rate of the instability over that which would result if the eigenfunction were not changed.

In Fig. 8 the growth rate with respect to the gap size is plotted, as in Fig. 2, but for 4 different values of the plasma wall separation ranging from $d/a = 1.05$ to $d/a = 1.20$. The graph shows that a closer wall compensates a lot towards having an outboard gap, but

not as much towards having a partial wall only on the outboard side. In other words, the smaller wall separations allow much larger outboard gaps for the same growth rates than the larger separations. The difference is not as large in the other sense (when there is only conducting wall on the outboard side).

III. Partial Walls With Rotation

Here, the ability of partial walls to stabilize the resistive wall mode with toroidal rotation will be considered. It is well established[5,6,14,15] that the resistive wall mode is more easily stabilized (i.e. stabilized at a lower rotation velocity) when the wall is farther away from the plasma. The reduced coupling of the mode to the resistive wall, when the wall is farther away, helps to stabilize the resistive wall mode. This suggests that it might also be easier to stabilize the resistive wall mode if there are gaps in the wall. In other words, a partial wall at a given plasma-wall separation might act similarly to a complete wall that is farther away. This was shown to be the case with toroidal gaps.[15] However, we have seen in the previous section that a gap on the outboard side, where the mode structure is concentrated, has a much larger effect on the growth rate than gaps placed elsewhere around the plasma. We shall see that outboard gaps have a strong favorable effect on the wall stabilization by rotation of pressure-driven kinks, and that such gaps can greatly relax the requirements of rotation velocity and/or wall separation at the expense of requiring a smaller wall separation in order to stabilize the ideal plasma mode.

It has been shown[6,7,14,15] that some kind of plasma dissipation is needed to stabilize the resistive wall mode. In these calculations the effect of Landau damping of the sound waves is modeled using a fluid approximation. In order to approximate the effect of the Landau damping of sound waves in the plasma, the perturbed pressure is split into a convective and a Lagrangian part,

$$p_1 = -\vec{\xi} \cdot \nabla p_0 + p_{1L} \tag{1}$$

where

$$\partial p_{1L}/\partial t = -\Gamma p_0 \nabla \cdot \vec{v} - \nu p_{1L} \tag{2}$$

The damping rate ν is taken to be a constant in the calculations presented here. This is one of the approximations used in Refs. 5 and 6.

In Fig. 9 we plot the growth rate normalized to the wall time, $\gamma\tau_w$ vs. the wall separation, d/a, for the high-beta, reversed-shear equilibrium used earlier, with a poloidally continuous resistive wall compared to a section of the wall with the inboard wall missing 75% of the way to the outboard midplane (i.e., only the outboard 25% of the wall remains)—at fixed rotation frequency, $\omega_r/\omega_A = 0.10$. The results show that the case with only a partial wall stabilizes more easily, i.e., with the wall closer to the plasma. Therefore by introducing a very large gap on the inboard side, it is effectively like moving the wall somewhat farther from the plasma in terms of stabilizing the resistive wall mode. Of course, this makes stabilization against the plasma mode somewhat more difficult, in that the marginal wall separation for stability to the ideal plasma mode is closer to the plasma, but in this case the change is not very great since the outboard wall section provides most of the stabilization and the inboard section very little.

Figure 10 shows the same cases for fixed wall position ($d/a = 1.04$) in terms of rotation frequency, ω_r, needed to stabilize the resistive wall mode. Removing the inboard section of the resistive wall allows stabilization at a rotation frequency about 6% lower than with a complete resistive wall at the same wall separation.

The results from Section II demonstrate that the pressure-driven kink mode couples most strongly to the wall on the outboard side. Therefore, since the resistive wall mode is more easily stabilized by reducing the coupling to the wall, it makes sense that by introducing a gap on the outboard side, and thereby removing the section of the wall to which the mode couples most strongly, it would be much easier to stabilize the resistive wall mode.

Figure 11 shows the results with a wall separation of $d/a = 1.04$ and a gap centered at

the *outboard* midplane with half-width $\theta_g = 0.2\pi$. The two curves represent two values of the pressure-damping coefficient ν, from Eq. (2), differing by a factor of 5. For both values of ν, the threshold rotation frequency above which the resistive wall mode is stabilized is $\omega_r/\omega_A \approx 0.103$—a reduction of 13% from the case with a full wall.

Figure 12 shows result for a somewhat larger outboard gap of half-width $\theta_g = 0.27\pi$, again for two values of ν (here differing by a factor of 2). Here the threshold rotation frequency is $\omega_r/\omega_A \approx 0.092$ for both values of ν—a 22% reduction from the case with a full wall.

It is quite noticeable that in all four curves of Figs. 11 and 12, that there is some stabilization at intermediate frequencies as well. For the curve with $\nu = .1$ at $\theta_g = 0.2\pi$ in Fig. 11, there is just a shallow dip in γ with a minimum at $\omega_r/\omega_A \approx 0.081$. However, at the lower damping coefficient of $\nu = .02$ the dip extends to negative values of γ and a very narrow band of stable frequencies exists at $\omega_r/\omega_A \approx 0.081$ with width $\Delta\omega_r/\omega_r \approx .002$.

With a larger outboard gap this band of stabilization is widened. Figure 12 shows that this dip in the $\nu = .1$ curve drops down to marginally stable values. The curve for $\nu = .05$ shows a larger gap than for the case in Fig. 11, although the gap is still relatively narrow.

The magnitude of the band of stable values for ω_r—even whether it exists at all—is a strong function of the damping coefficient, ν. And yet the value of the true threshold for rotation frequency which stabilizes the mode (beyond which the resistive wall modes remains stable) does not seem to be strongly affected by the value of the damping coefficient as can be seen in Figs. 11 and 12.

However, the existence of this narrow band is not a particularly significant effect, in that it exists only for a small range of values for the gap width, θ_g, and the band itself is quite narrow in terms of stable values of ω_r. Figure 13 shows the results for a slightly larger gap of $\theta_g = 0.3\pi$, along with the results for $\theta_g = 0.27\pi$, $\theta_g = 0.2\pi$, and $\theta_g = 0$ (full wall). Here we see that the narrow band of stable values of ω_r has vanished when $\theta_g = 0.3\pi$, since the

outer threshold value has moved to the left in the figure past the gap. The band of stable values does not move in the direction of lower ω_r as fast as the stability threshold point, therefore the band of stable ω_r's vanishes as the magnitude of the outboard gap increases.

The phenomenon of a range of stable values in ω_r below the real threshold value for stability is not a result of the existence of gaps in the wall. Figure 14 shows γ vs. ω_r for several values of wall separation d/a, but with a poloidally continuous and complete wall. It can be seen that there is a narrow range of stable values centered around $\omega_r/\omega_A \approx 0.08$ for $d/a = 1.26$. The mode becomes unstable again at higher values of ω_r/ω_A and finally stabilizes at $\omega_r/\omega_A \approx 0.093$. For a plasma-wall separation of $d/a = 1.28$ there is a somewhat larger range of values of ω_r/ω_A centered at $\omega_r/\omega_A \approx 0.077$, which becomes unstable again at $\omega_r/\omega_A \approx 0.084$, and then stabilizes at the threshold value of $\omega_r/\omega_A \approx 0.089$. At larger wall separations (e.g., $d/a = 1.30$) there is no range of stable values below the threshold value ($\omega_r/\omega_A \approx 0.066$ at $d/a = 1.30$).

Figure 13 shows that the threshold value of stability of ω_r for the case with an outboard gap of $\theta_g = 0.3\pi$ is $\omega_r/\omega_A \approx 0.069$. This is a reduction of 41% of the necessary rotation frequency to stabilize compared to the case with a full wall. The necessary wall separation needed to stabilize the ideal plasma mode is $d/a = 1.06$ for the case with an outboard gap of $\theta_g = 0.3\pi$, compared to $d/a = 1.36$ for the full wall. This results in the need to have the wall somewhat closer when there is such a gap, but there is a significant reduction in the necessary rotation to stabilize the resistive wall mode.

A. Wall Stabilization with Discrete Conducting Plates

In the TPX design[20] passive stabilization against the axisymmetric, vertical instability and against ideal external kinks[21] is provided by conducting plates on the inboard and outboard sides. In fact, the passive structure is not quite axisymmetric and actually takes the form of a 3-dimensional "cage".[21] But it can be approximated as two pairs of axisymmetric

plates. As we have seen that a resistive wall on the inboard side has very little effect on the kink mode in high-pressure, reversed-shear equilibria, the inboard plates will be ignored in the following calculations. These calculations use a pair of conformal wall sections on the outboard side with the same poloidal angular extent as the outboard TPX plates (from $|\theta| = 0.18\pi$ to $|\theta| = 0.48\pi$).

The results are shown in Fig. 15. The growth rates are normalized to the same wall time (calculated for a complete resistive wall) as in Fig. 10. Here we see that the growth rates are considerably higher than for the cases in Fig. 10, particularly in the peak just short of the critical growth rate for stabilization. But we see that stabilization occurs at a much lower rotation frequency. In fact, the necessary critical frequency for stabilization is reduced by a factor of approximately 3.6 compared to the case with a complete wall with the same plasma-wall separation (with a full wall at $d/a = 1.04$ there is stabilization at $\omega_\tau/\omega_A \approx .12$).

By comparing the curves in Figs. 10 and 15 we see the effect of reducing the coverage of the wall on the resistive wall mode. As the amount of conducting coverage decreases the overall growth rate goes up, as one would expect. Also, the peak in the growth rate just below the critical rotation frequency, ω_c, becomes much narrower, steeper, and greater in magnitude. In the case of the approximation to the TPX plates, the growth rate is larger by well over an order of magnitude compared to the case with a full resistive wall. Therefore, if the rotation velocity is short of the critical value then the mode growth rate will be very much higher with the limited coverage of the plates. But the necessary rotation required for complete stabilization is much less for the case with discrete conducting plates than for the full wall.

Of course, the other great effect is on the critical wall position for stabilizing the ideal plasma mode. For the calculations shown in Fig. 15, the plasma-wall separation for the conformal plates was $d/a = 1.04$. The critical wall separation for marginal stability for the ideal plasma mode is $d/a = 1.07$. This is greatly reduced from the critical value with

a full wall of $d/a = 1.36$. This leaves a very narrow region of stability for the position of the plates. Therefore, there is a trade-off by removing sections of the wall and using only plates of limited poloidal extent instead of a full resistive wall.

Let us compare the region of stability (in terms of wall position) for a full wall: $d/a = 1.24 - 1.36$ at $\omega_\tau/\omega_A = 0.10$ to that with the approximation of the TPX plates: $d/a = 1.04 - 1.07$ at $\omega_\tau/\omega_A = 0.0328$. The extent of the region of stability in terms of wall position is greatly reduced, and is shifted much closer to the plasma. However, the critical rotation frequency, ω_c, to stabilize the resistive wall mode is greatly reduced—by over a factor of 3 in this case. This can be a very advantageous trade-off since it may be difficult to maintain the high rotation frequencies that were required for stabilization of this equilibrium in Ref. 6 (as much as 10% of the Alfvén frequency) in an experiment. Also, for a realistic design it is very often necessary to have a large midplane gap on the outboard side in the close-fitting passive conductors in order to allow access for diagnostics and neutral beams. Therefore, the existence of a realistic outboard gap in the resistive wall allows the region of stability for the resistive wall mode (in terms of wall position and rotation velocity) to be shifted to a much more accessible domain, even when the overall extent of the region of stability (in terms of wall position) is smaller.

IV. Summary and Discussion

The effect of toroidally continuous gaps in the resistive wall on the stability of low-n external kink modes has been examined both with and without toroidal rotation. These gaps in the resistive wall can significantly increase the growth rate of low-n kink modes. This is particularly true of outboard gaps for pressure-driven kink modes, because of the concentration of the mode structure on the outboard side. Removing the wall on the inboard side has relatively little effect on such modes. In addition, the form of the eigenfunction of the displacement is modified in response to the placement of these gaps. The eigenfunction

changes in such a way that the stabilizing eddy currents are pushed into the gap and out of the remaining conductor. This reduces the stabilizing effect and increases the growth rate.

For the stabilization of resistive wall modes by toroidal rotation, the gaps can have a beneficial effect. The presence of gaps has the same stabilizing effect as moving the wall away from the plasma. Of course, gaps in the region of the wall where there is the greatest coupling to the wall have the largest effect. Thus, for pressure-driven kink modes, gaps on the inboard side have little effect, whereas those near the outboard midplane can greatly relax the requirements for minimum rotation speed or minimum wall separation necessary to stabilize the resistive wall mode. This is done, however, at the expense of requiring a much smaller wall separation to stabilize the ideal plasma mode, because of the reduced stabilization by the wall as described above. But this trade-off can be quite favorable if the necessary rotation velocity is greatly reduced by the presence of the gap—especially in designs where an outboard gap in the close fitting passive conductors is necessary anyway for technical or engineering reasons.

Recent analysis of PBX-M data demonstrates wall stabilization of pressure driven modes.[12] Analysis of the reconstructed shot equilibrium shows that the plasma beta is above the ideal MHD beta limit with the wall at infinity, but stable with a close fitting ideal wall. Calculations[12] were done with the NOVA-W code, using the actual form the the PBX-M wall including the large gap at the outboard midplane, showed that the resistive wall mode could be stabilized at approximately the rotation speeds that were measured in the experiment. These calculations also indicated that the necessary toroidal rotation speed was reduced by over a factor of two compared to that which would be needed if the PBX-M wall had no gaps. This significant reduction in the necessary rotation speed owing to the outboard gap, which is a integral part of the design, allowed stabilization of the instability at rotation speeds that are attainable in the PBX-M experiment.

While the precise quantitative results presented here have some dependence on the model used to simulate the sound wave damping, Eq. (2), and quantitative results might

differ somewhat with other models as in Ref. 6, the same reduction in the rotation frequencies needed to stabilize the resistive wall mode in the presence of gaps in the wall (and likewise the same reduction in allowable plasma-wall separation to stabilize the ideal plasma mode) will be seen regardless of the mechanism used for dissipation. In fact, since the dependence on the wall separation for stabilization of resistive wall modes is common to all of the recent theories, this effect would also be present in theories with a completely different mechanism for stabilization.[22,23]

The improvements in resistive wall mode stability described here may even be applicable to tokamak designs with a completely surrounding wall such as ITER.[24] If it is possible to design the wall modules in ITER such that the eddy current paths were interrupted near the outboard midplane (i.e., making a very high effective resistivity in a limited part of the outboard wall) where the high-β kink couples the strongest to the wall, then the same effect would be seen. This would cause very little degradation to vertical stability, because the axisymmetric vertical mode is almost completely antisymmetric and therefore couples very little to the wall near the outboard midplane.[19]

Acknowledgments

This research was funded in part by the Fonds National Suisse pour la Recherche Scientifique.

References

[1]F. Troyon, R. Gruber, H. Saurenmann, S. Semenzato, S. Succi, Plasma Phys. Controlled Fusion **26**, 209 (1984).

[2]E. J. Strait, Phys. Plasmas **1**, 1415 (1994).

[3]Z. Yoshida and N. Inoue, Plasma Phys. Controlled Fusion **27**, 245 (1985).

[4]L. E. Zakharov and S. V. Putvinskii, Sov. J. Plasma Phys. **13**, 68 (1987).

[5]A. Bondeson and D. J. Ward, Phys. Rev. Lett. **72**, 2709 (1994).

[6]D. J. Ward and A. Bondeson, Phys. Plasmas **2** 1570 (1995).

[7]R. Betti and J. P. Freidberg, Phys. Rev. Lett. **74** (1995) 2949.

[8]A.D. Turnbull, T.S. Taylor, E.J. Strait, S.J. Thompson, M.S. Chu, J.R. Ferron, R. J. La Haye, L.L. Lao, R.T. Snider, B. Rice, D. Wròblewski, O. Sauter, M. E. Mauel, A. Popov, N. Popova, D. J. Lightly, J. D. Williams, in Plasma Physics and Controlled Nuclear Fusion Research 1994, Proc. 15th Int. Conf., Seville (International Atomic Energy Agency, Vienna, 1995) Vol. 1, p. 705.

[9]E. J. Strait, T. S. Taylor, A. D. Turnbull, J. R. Ferron, L. L. Lao, B. W. Rice, O. Sauter, S. J. Thompson, and D. Wròblewski, Phys. Rev. Lett., **74** 2483 (1995).

[10]T. S. Taylor, E. J. Strait, L. L. Lao, M. Mauel, A. D. Turnbull, K. H. Burrell, M. S. Chu, J. R. Ferron, R. J. Groebner, R. J. La Haye, B. W. Rice, R. T. Snider, S. J. Thompson, D. Wròblewski, D. J. Lightly, Phys. Plasmas, **2** 2390 (1995).

[11]M. S. Chu, J. M. Greene, T. H. Jensen, R. L. Miller, A. Bondeson, R. W. Johnson, M. E. Mauel, Phys. Plasmas **2** (1995) 2236.

[12]M. Okabayashi, N. Pomphrey, J. Manickam, D. Ward, R. Bell, R. Hatcher, R. Kaita, S. Kaye, H. Kugel, B. LeBlanc, F. Levinton, D. Roberts, S. Sesnic, Y. Sun, and H. Takahashi, "Role of the Stabilizing Shell in High-β / Low-q Disruptions in PBX-M," PPPL-3168, January, 1996; submitted to Nucl. Fusion.

[13]T. H. Ivers, E. Eisner, A. Garofalo, D. Gates, R. Kombargi, M. E. Mauel, D. Maurer, D. Nadle, G. A. Navratil, M. K. V. Sankar, and Q. Xiao, paper CN-60-A-3/5-P-15. in Plasma Physics and Controlled Nuclear Fusion Research 1994, Proc. 15th Int. Conf., Seville (International Atomic Energy Agency, Vienna, 1995).

[14]N. Pomphrey, S. C. Jardin, J. Bialek, M. S. Chance, D. A. D'Ippolito, J. M. Finn, R. Fitzpatrick, J. L. Johnson, C. E. Kessel, J. Manickam, D. A. Monticello, J. R. Myra, M. Ono, W. Park, A. Reiman, G. Rewoldt, W. M. Tang, E. J. Valeo, and L. E. Zakharov, in Plasma Physics and Controlled Nuclear Fusion Research 1994, Proceedings of the 15th International Conference, Seville (International Atomic Energy Agency, Vienna, in press), Paper No. IAEA-CN-60/D-I-14.

[15]R. Fitzpatrick and A. Aydemir, "Stabilization of the Resistive Shell Mode in Tokamaks," IFSR-#694, Feb. 1995, University of Texas, Austin. Submitted to Nucl. Fusion.

[16]D. J. Ward, S. C. Jardin, and C. Z. Cheng, J. Comp. Phys. **104**, 221 (1993).

[17]C. Z. Cheng and M. S. Chance, J. Comp. Phys. **71**, 124 (1987).

[18]C. Kessel, J. Manickam, G. Rewoldt, and W. M. Tang, Phys. Rev. Lett. **72**, 1212 (1994).

[19]D. J. Ward, S. C. Jardin, Nucl. Fusion **32**, 973 (1992).

[20]R. J. Goldston, G. H. Neilson, K. I. Thomassen, D. B. Batchelor, P. T. Bonoli, J. N. Brooks, R. Bulmer, M. E. Fenstermacher, D. N. Hill, A. Hubbard, E. F. Jaeger, S. Jardin, C. Kessel, R. La Haye, S. L. Liew, J. Manickam, T. K. Mau, D. Mikkelsen, P. Moroz, W. M. Nevins, L. D. Pearlstein, L. J. Perkins, P. A. Politzer, N. Pomphrey, M. Porkolab, J. Ramos, W. T. Reiersen, A. Reiman, G. Rewoldt, T. D. Ronglien,

D. N. Ruzic, J. E. Scharer, J. A. Schmidt, J. C. Sinnis, D. P. Stottler, W. Tang, M. Ulrickson, C. Wang, K. A. Werley, G. Wurden, and L. Zakharov, Controlled Fusion and Plasma Physics, Proceedings of the 20th European Conference, Lisboa, 1993 (European Physical Society, Petit-Lancy, Switzerland, 1993), Vol. 17C, Part I, p. 319.

[21]M. S. Chance, in Proc. 1995 International Sherwood Fusion Theory Conference, Incline Village, NV, April 1995.

[22]Allen H. Boozer, Phys. Plasmas **2** 4521 (1995).

[23]John M. Finn, Phys. Plasmas **2** 198 (1995).

[24]K. Tomabechi, J. R. Gilleland, Yu. A. Sokolov, R. Toschi, and the ITER Team, Nucl. Fusion **31** 1135 (1991).

Figures

FIG. 1. The geometry of outboard and inboard toroidally continuous gaps. In the following figures, a negative value of θ denotes a gap at the outboard side and a positive value denotes a gap on the inboard side.

FIG. 2. The growth rate normalized to the wall time with respect to the angular extent of the gaps on the inboard (positive θ) and outboard (negative θ) side.

FIG. 3. Plot of the magnitude of the induced currents in a complete resistive wall with respect to the normalized poloidal angle, s ($s = 0$ is at the outboard midplane).

FIG. 4. The growth rate normalized to the wall time with respect to the angular extent of the gaps on the inboard and outboard side for a $\beta = 0$ kink.

FIG. 5. Plot of the magnitude of the induced currents in a complete resistive wall with respect to the normalized poloidal angle, s, for the $\beta = 0$ kink ($s = 0$ is at the outboard midplane).

FIG. 6. Magnitude of the $m = 2, 3, 4$ harmonics of the eigenfunction at the plasma surface plotted together with the normalized growth rate ($\gamma\tau_w/20$) with respect to angular extent of gaps.

FIG. 7. The eddy currents for the case with a complete resistive wall (solid line—as in Fig. 3) plotted with those for the case with a large outboard gap (dashed line). The deformation in the eigenfunction is seen here to move the peak currents towards the gap.

FIG. 8. The growth rate normalized to the wall time with respect to the angular extent of the gaps on the inboard (positive θ) and outboard (negative θ) side for various wall separations, d/a.

FIG. 9. The effect of a large inboard gap on the resistive wall stabilization by rotation. The growth rates (normalized to the wall time) are plotted vs. wall separation, d/a, at fixed rotation speed, $\omega_r/\omega_A = 0.10$.

FIG. 10. The growth rates (normalized to the wall time) are plotted vs. the rotation frequency ω_r at fixed wall separation ($d/a = 1.04$).

FIG. 11. The growth rates (normalized to the wall time) are plotted vs. the rotation frequency ω_r at fixed wall separation ($d/a = 1.04$) for the case with and outboard gap of half-width $\theta_g = 0.2\pi$.

FIG. 12. The growth rates (normalized to the wall time) are plotted vs. the rotation frequency ω_r at fixed wall separation ($d/a = 1.04$) for the case with and outboard gap of half-width $\theta_g = 0.27\pi$.

FIG. 13. The growth rates are plotted vs. the rotation frequency ω_r at fixed wall separation ($d/a = 1.04$) for the cases with outboard gaps of half-widths $\theta_g = 0$ (full wall), $\theta_g = 0.2\pi$, $\theta_g = 0.27\pi$, and $\theta_g = 0.3\pi$.

FIG. 14. The growth rates are plotted vs. the rotation frequency ω_r at various wall separations with a complete and continuous wall to show that the existence of a stable band of frequencies below the threshold stabilizing frequency is not limited to cases with gaps in the wall.

FIG. 15. The growth rates (normalized to the wall time) plotted vs. ω_r for the case with plates of very limited poloidal extent, which are an axisymmetric approximation of the outboard plates in the TPX design.[20]

Figure 1

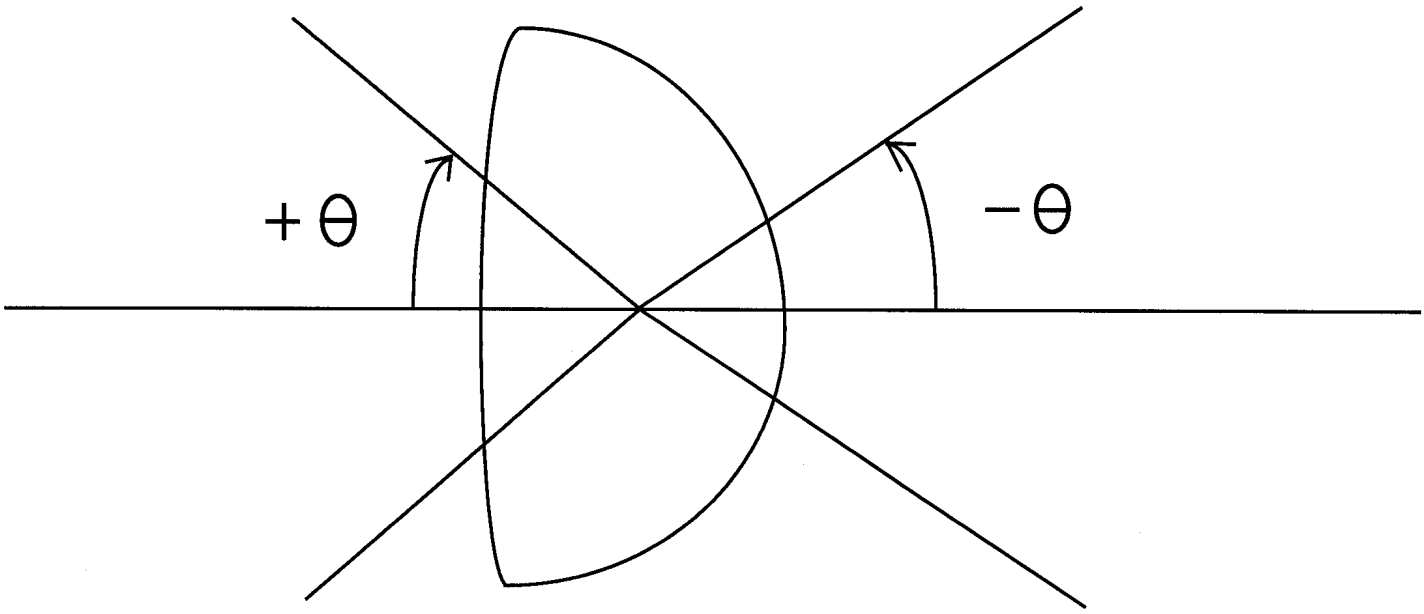

Figure 2

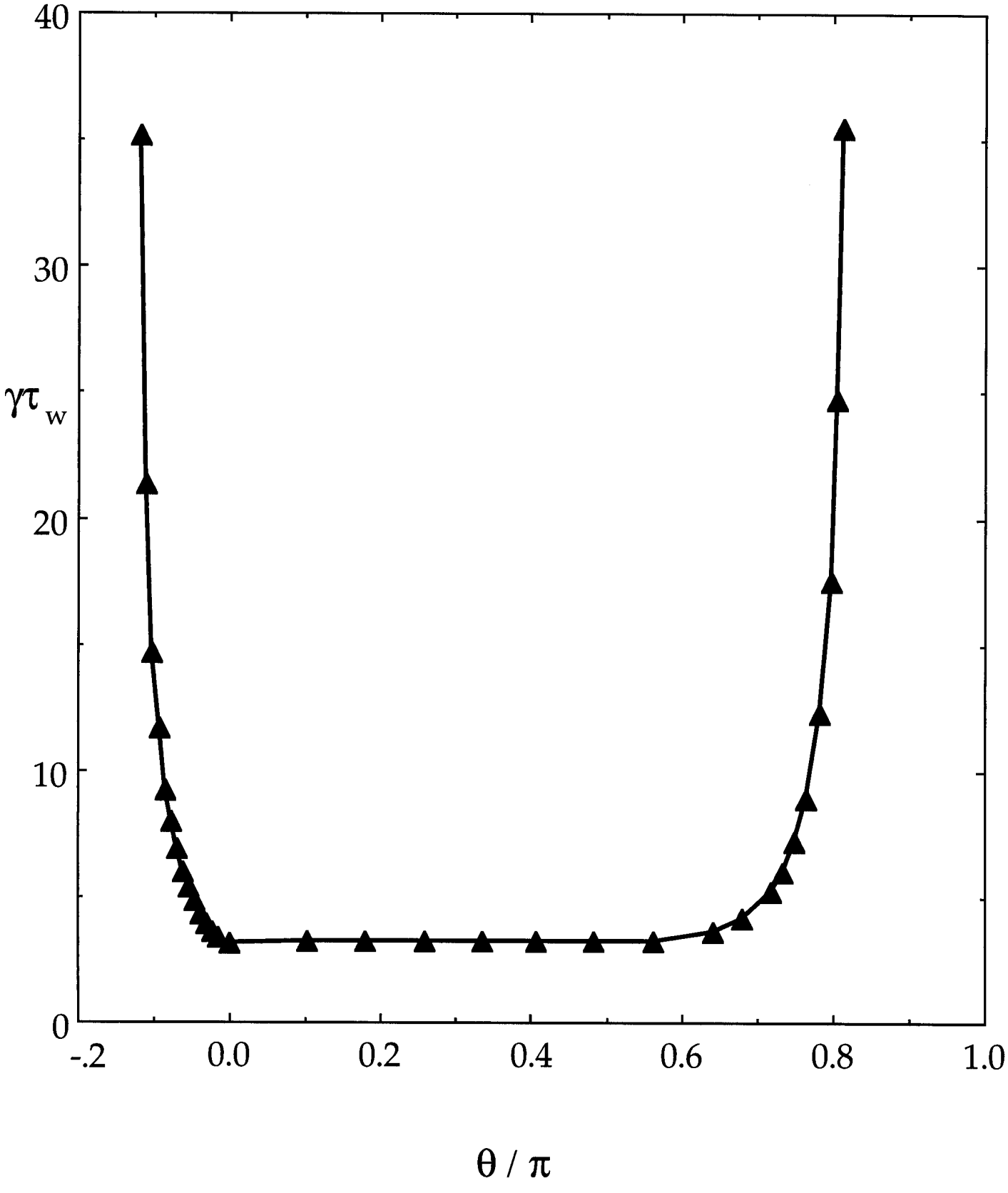

Figure 3

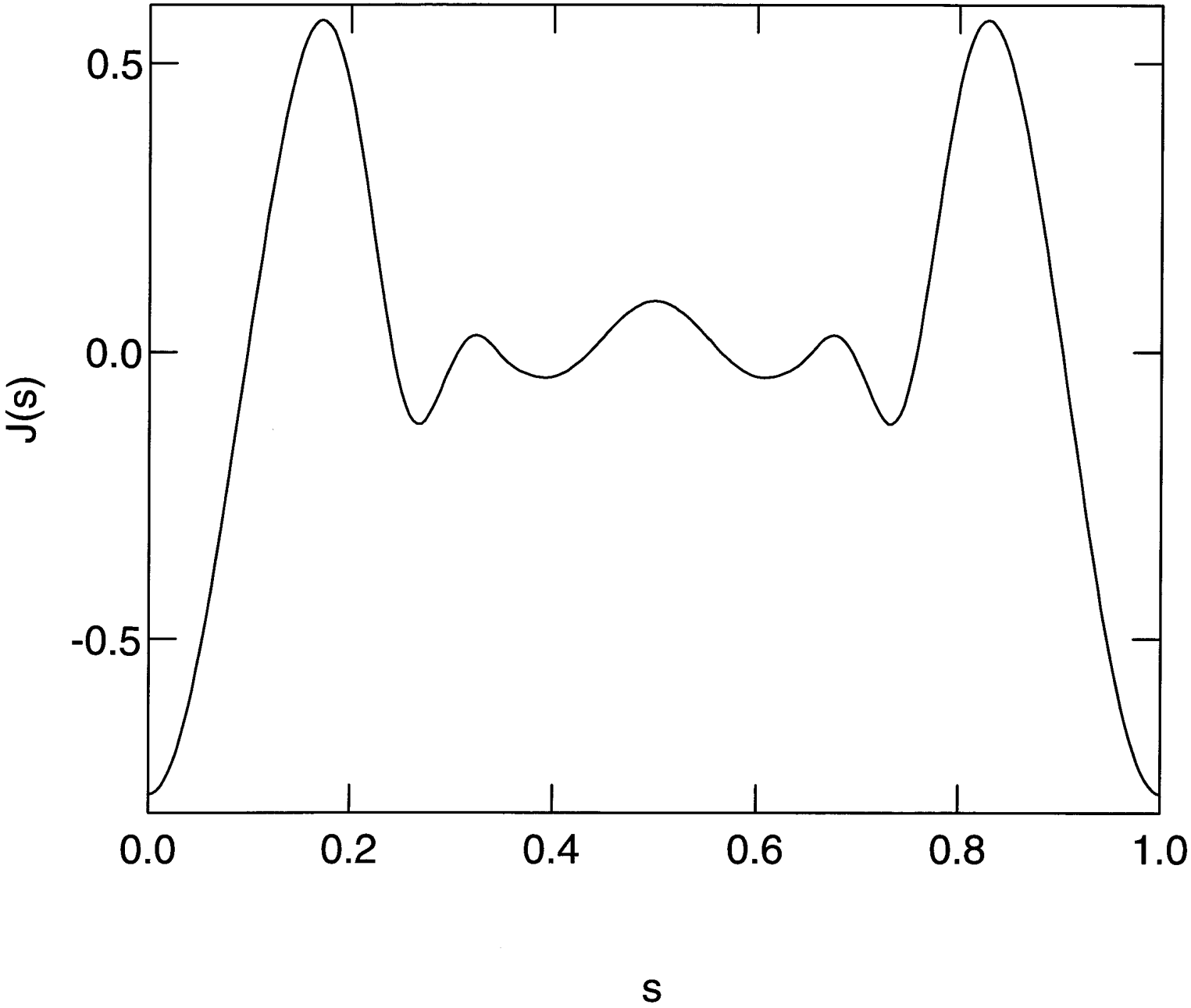

Figure 4

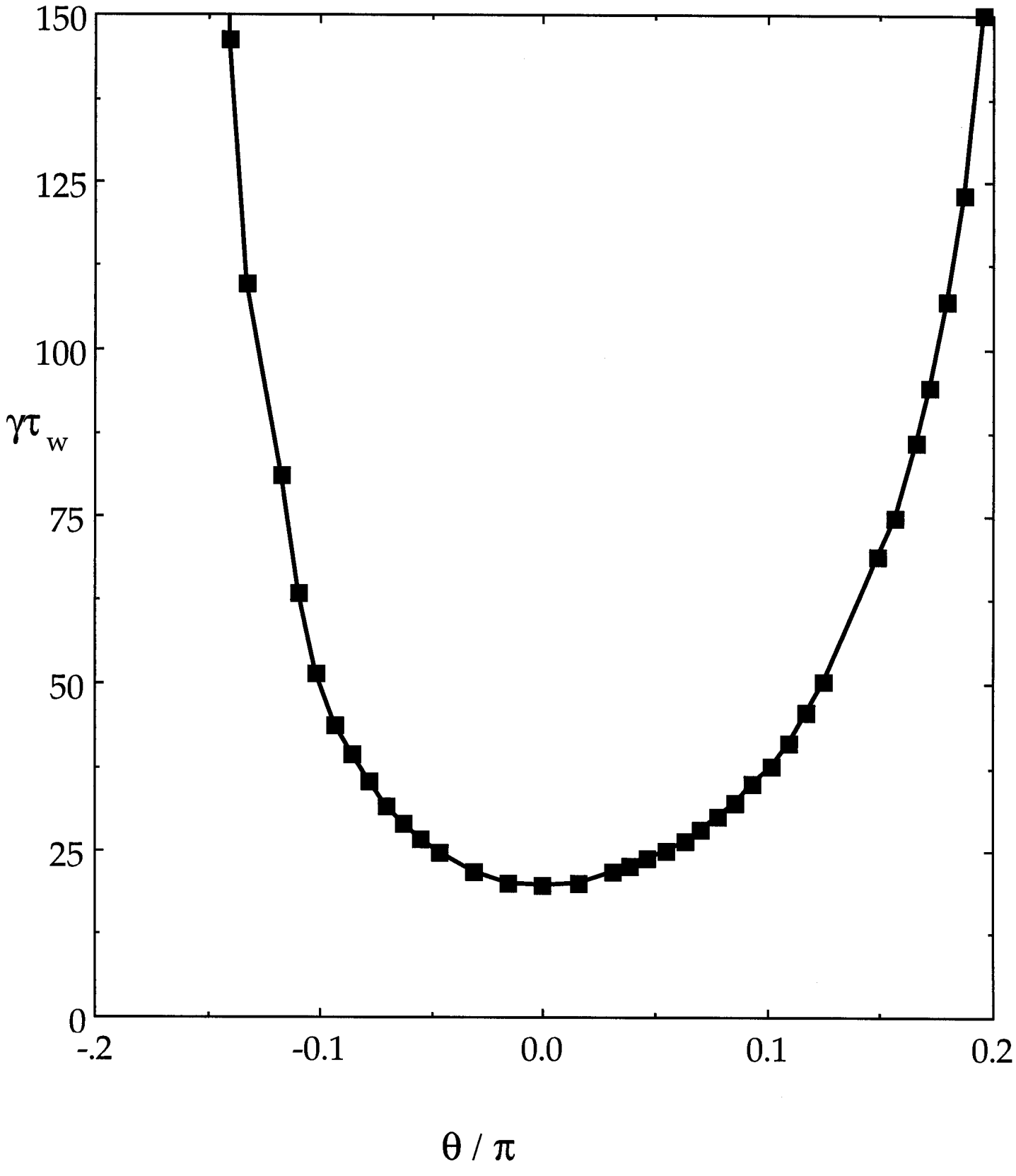

Figure 5

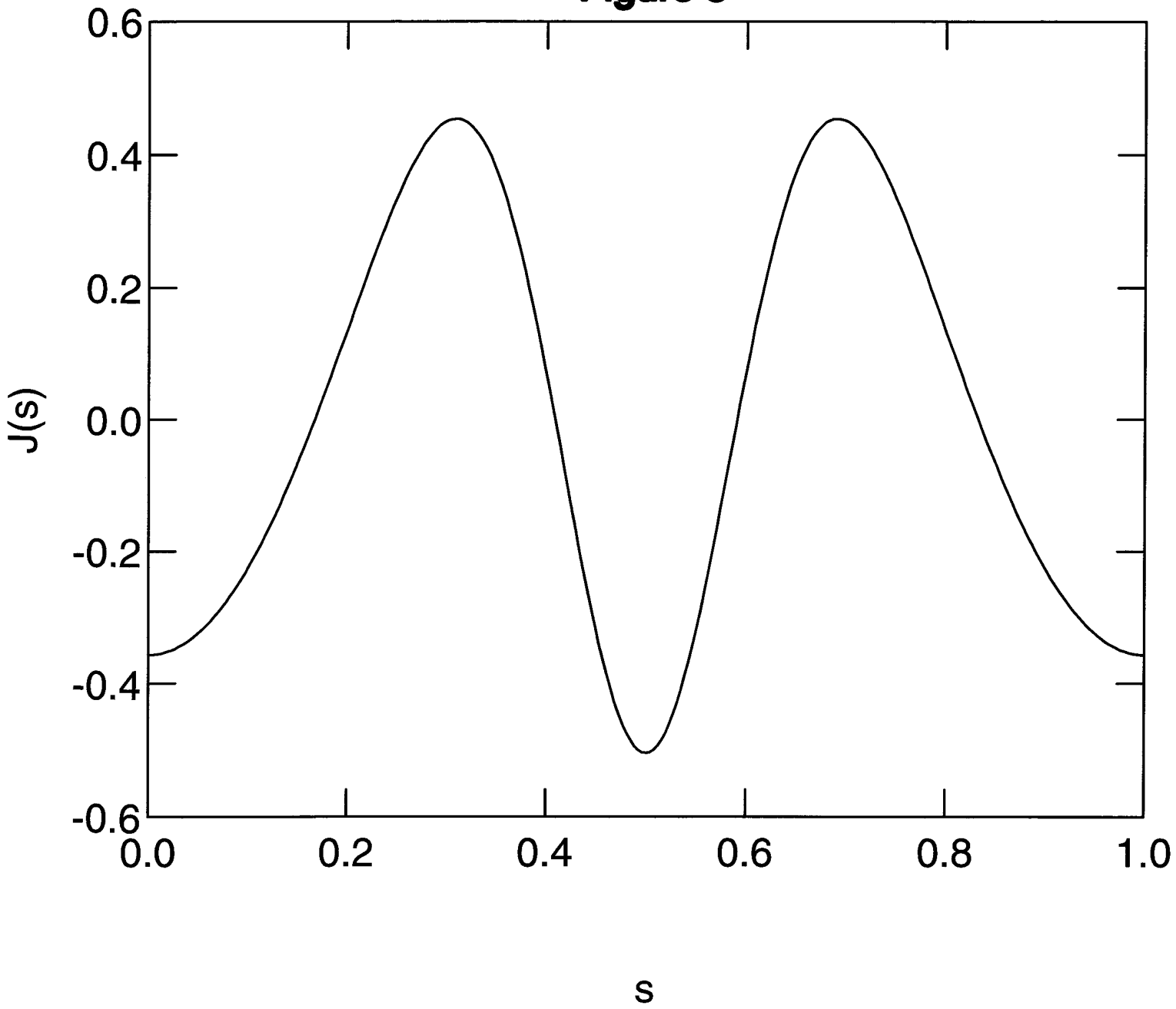

Figure 6

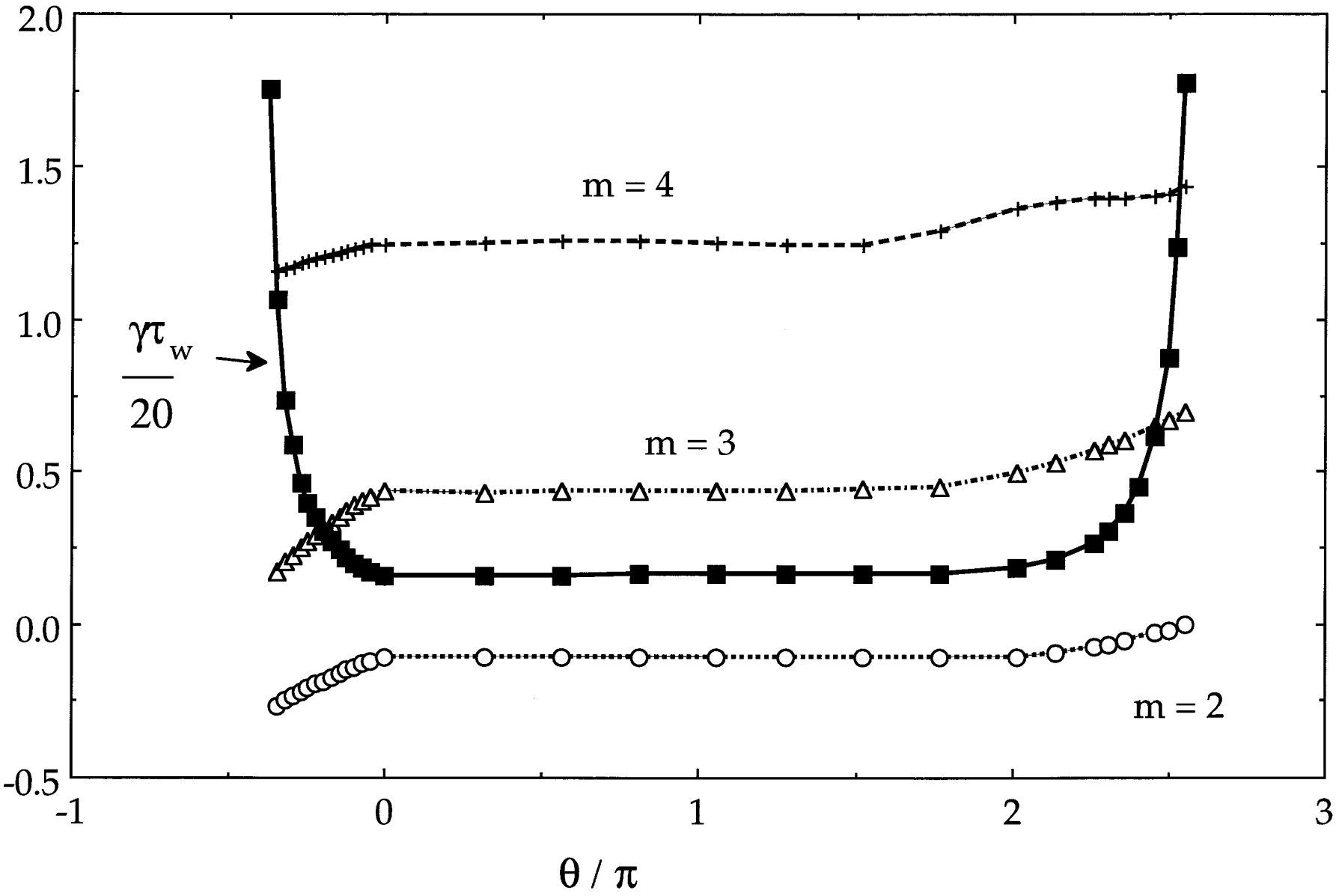

Figure 7

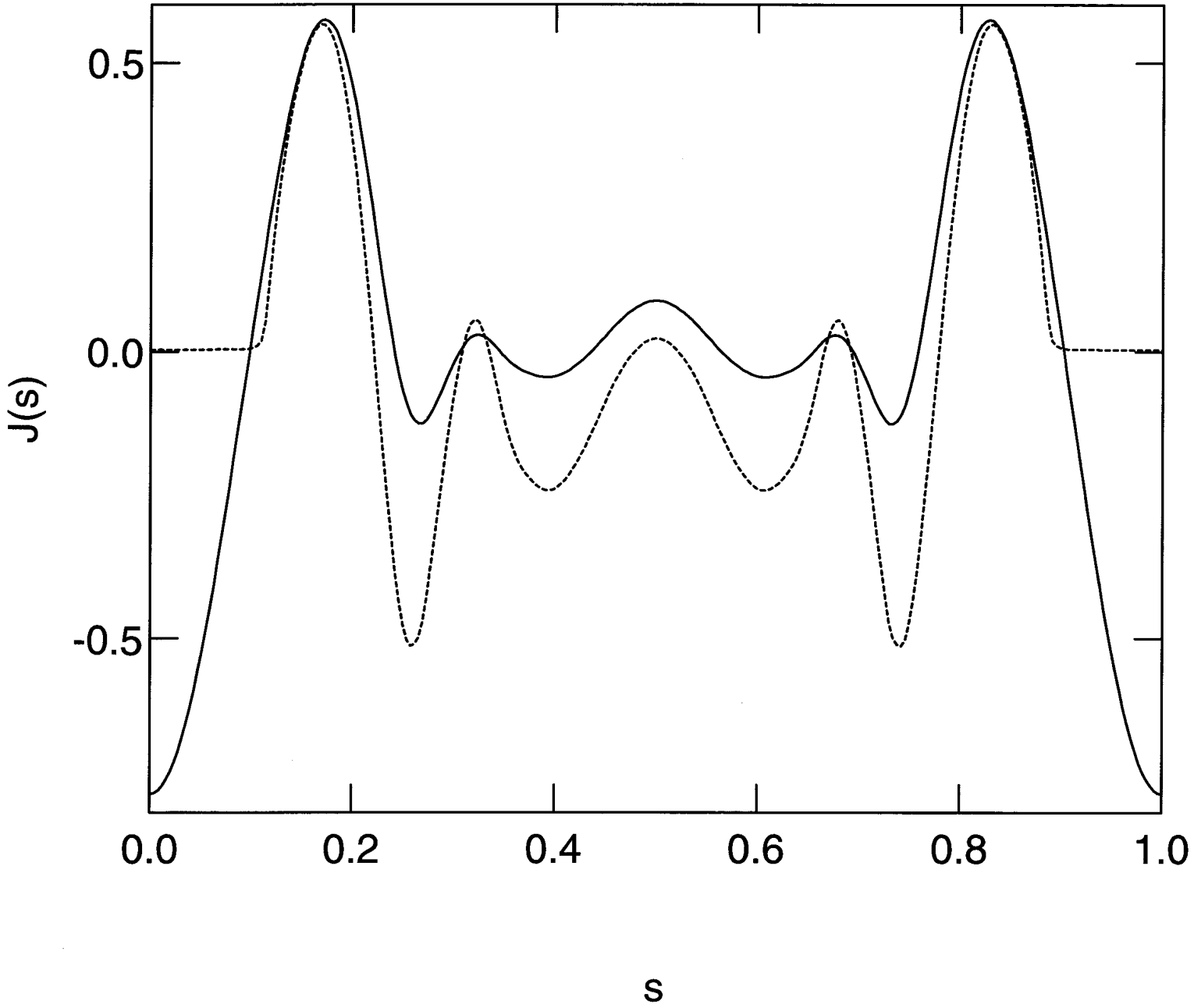

Figure 8

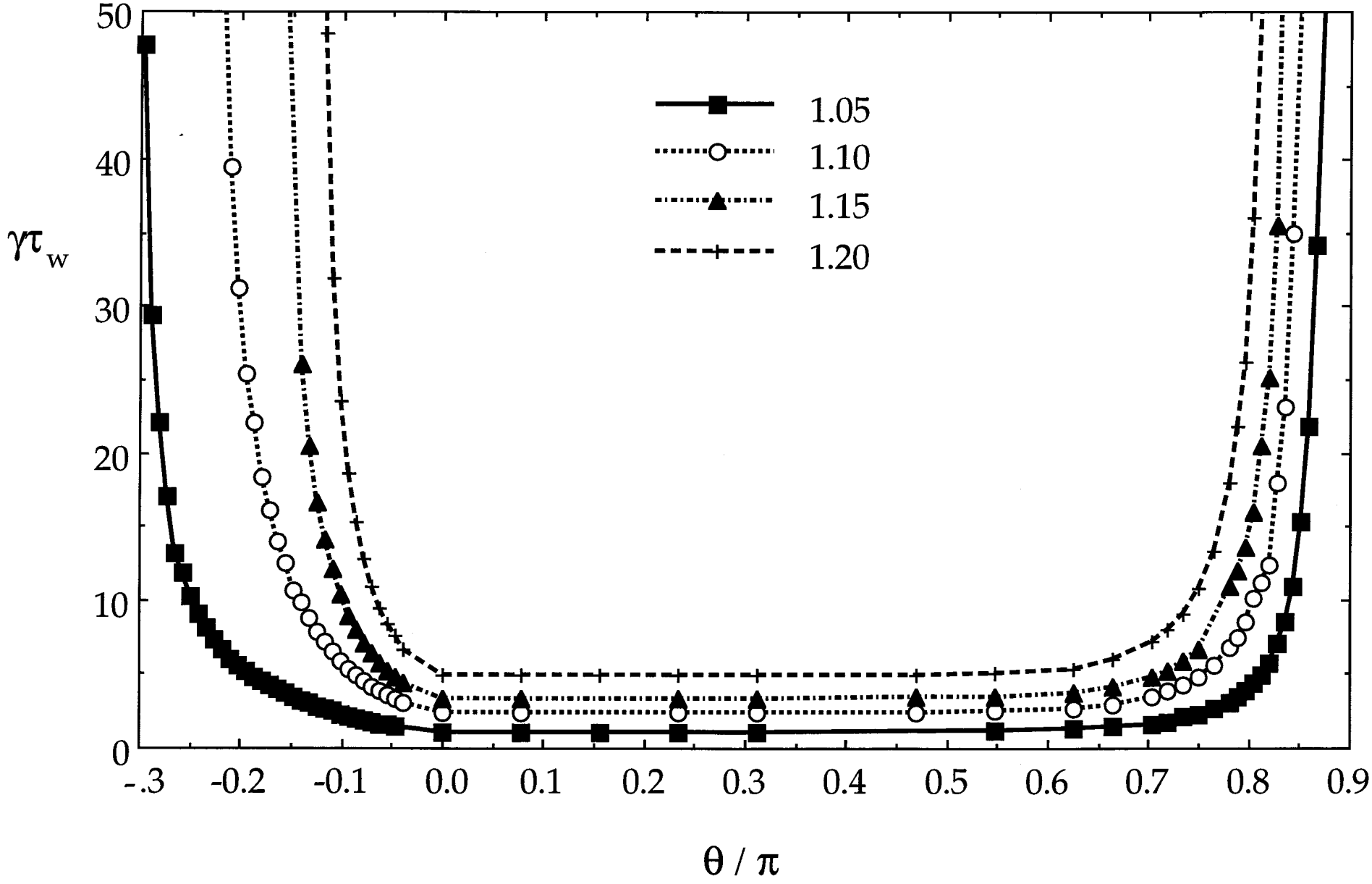
50
40
30
20
10
0
$\gamma\tau_w$
1.05
1.10
1.15
1.20
-.3
-0.2
-0.1
0.0
0.1
0.2
0.3
0.4
0.5
0.6
0.7
0.8
0.9
θ / π

Figure 9

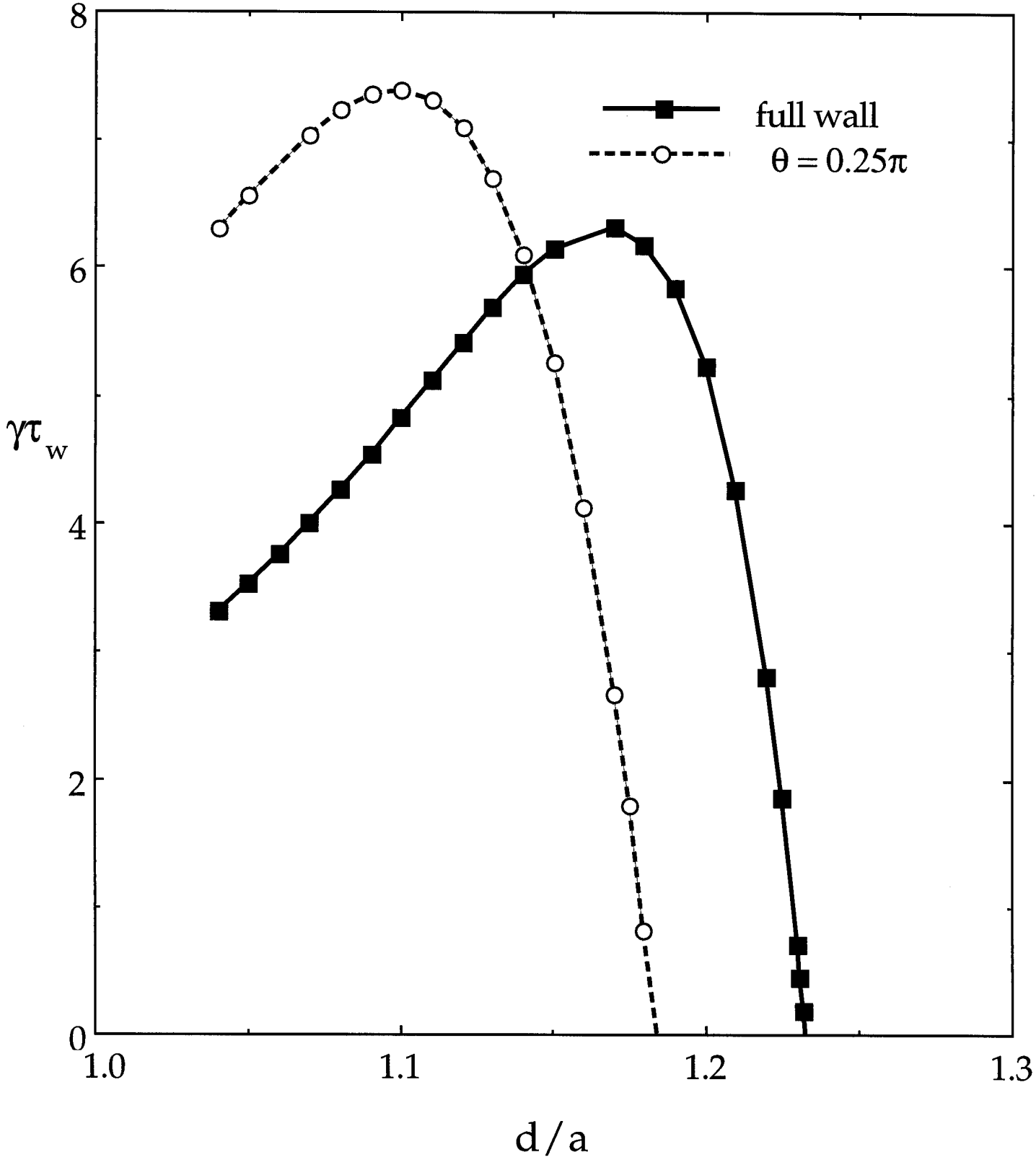

Figure 10

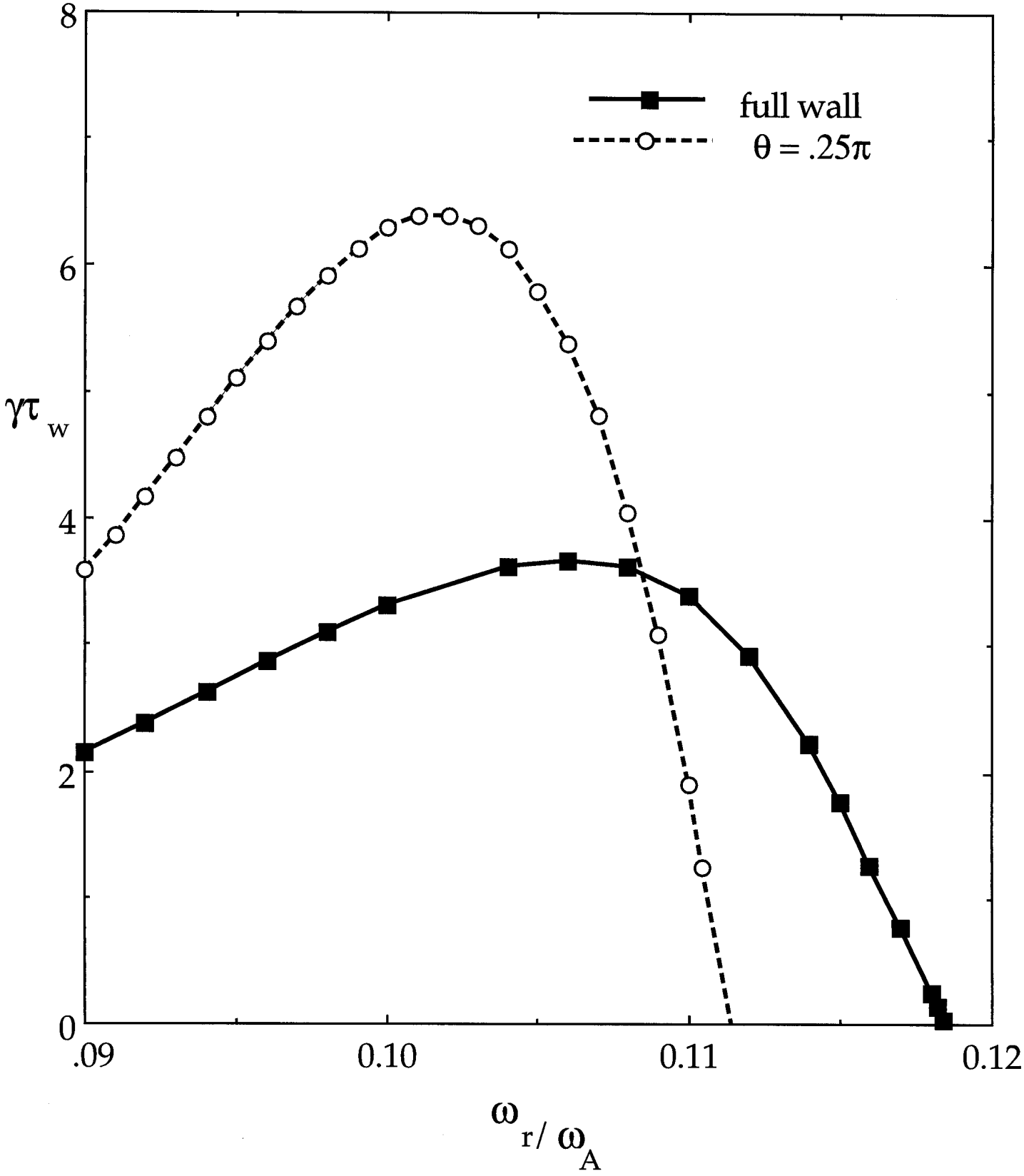

Figure 11

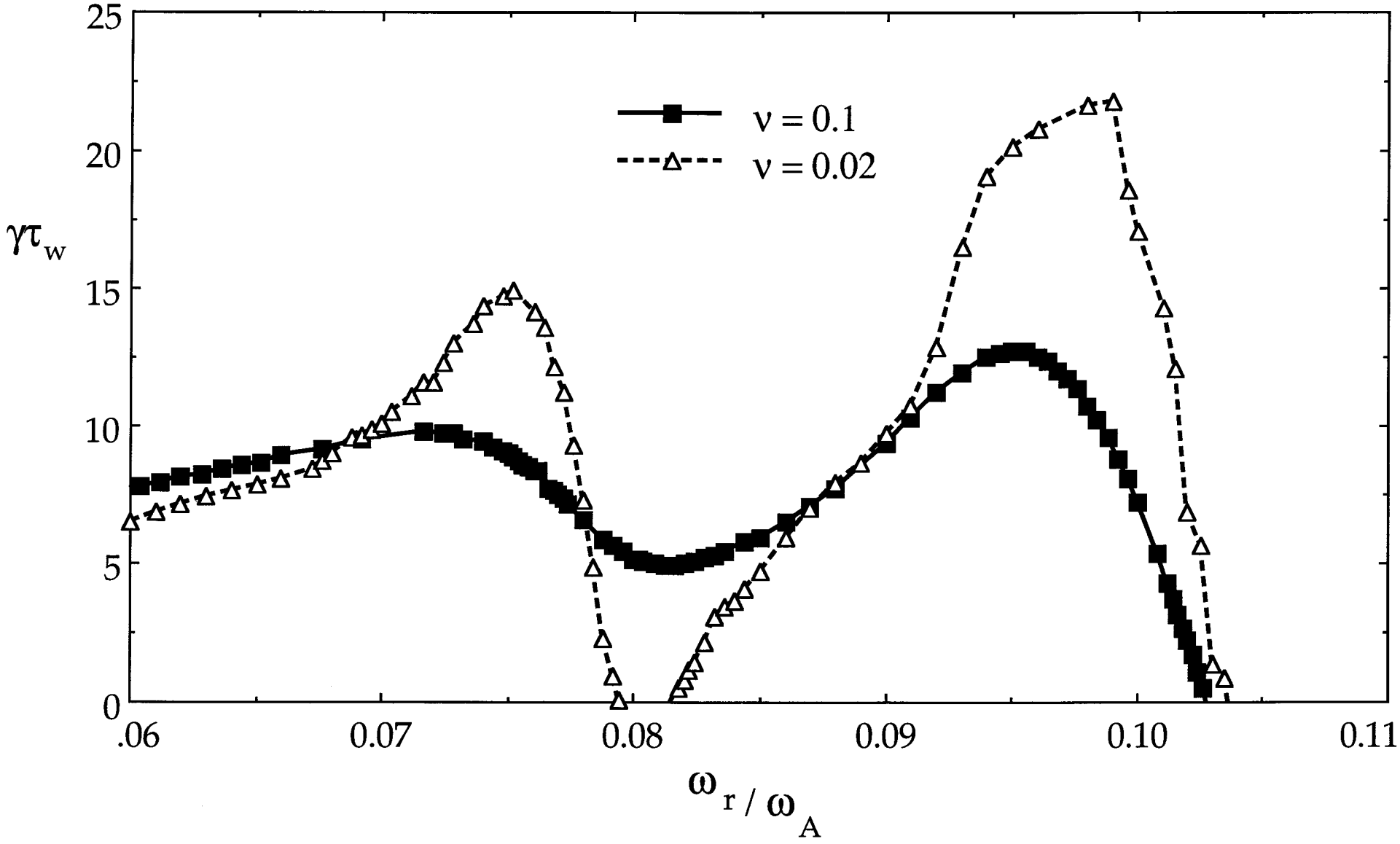
25
20
15
10
5
0
$\gamma\tau_w$
$\nu = 0.1$
$\nu = 0.02$
.06
0.07
0.08
0.09
0.10
0.11
ω_r / ω_A

Figure 12

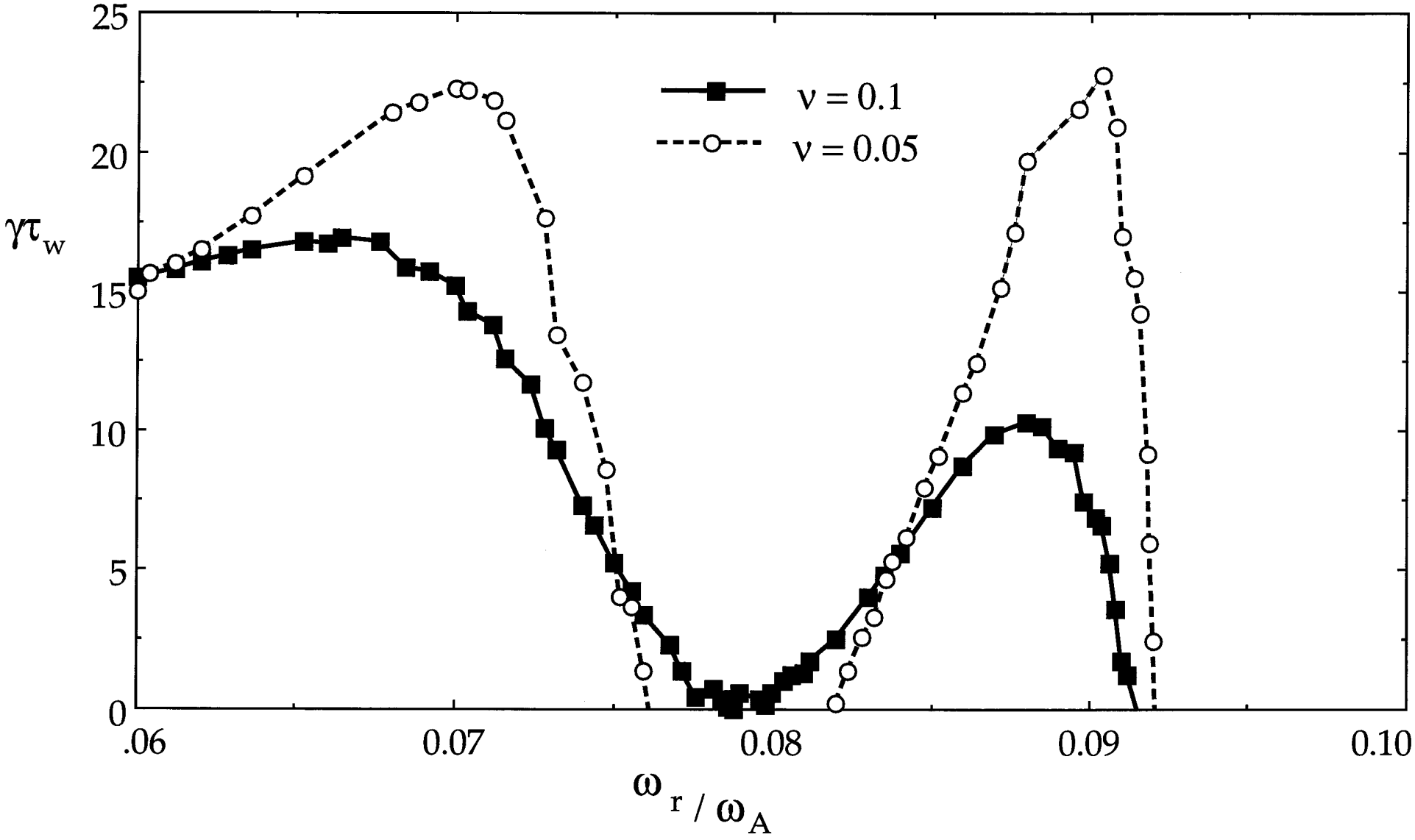
25
20
15
10
5
0
$\gamma\tau_w$
$\nu = 0.1$
$\nu = 0.05$
.06
0.07
0.08
0.09
0.10
ω_r / ω_A

Figure 13

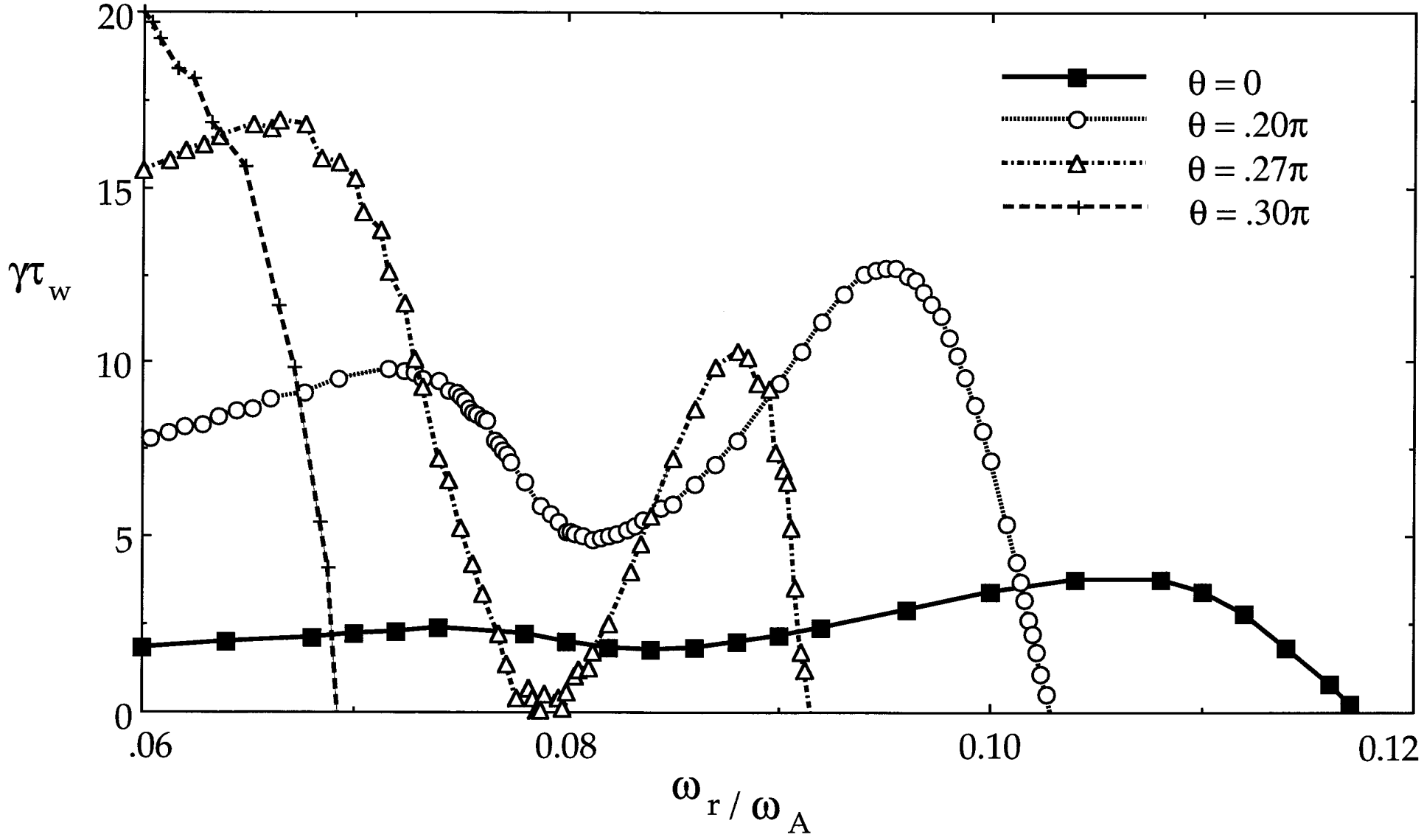
20
15
10
5
0
$\gamma\tau_w$
.06
0.08
0.10
0.12
ω_r / ω_A
$\theta = 0$
$\theta = .20\pi$
$\theta = .27\pi$
$\theta = .30\pi$

Figure 14

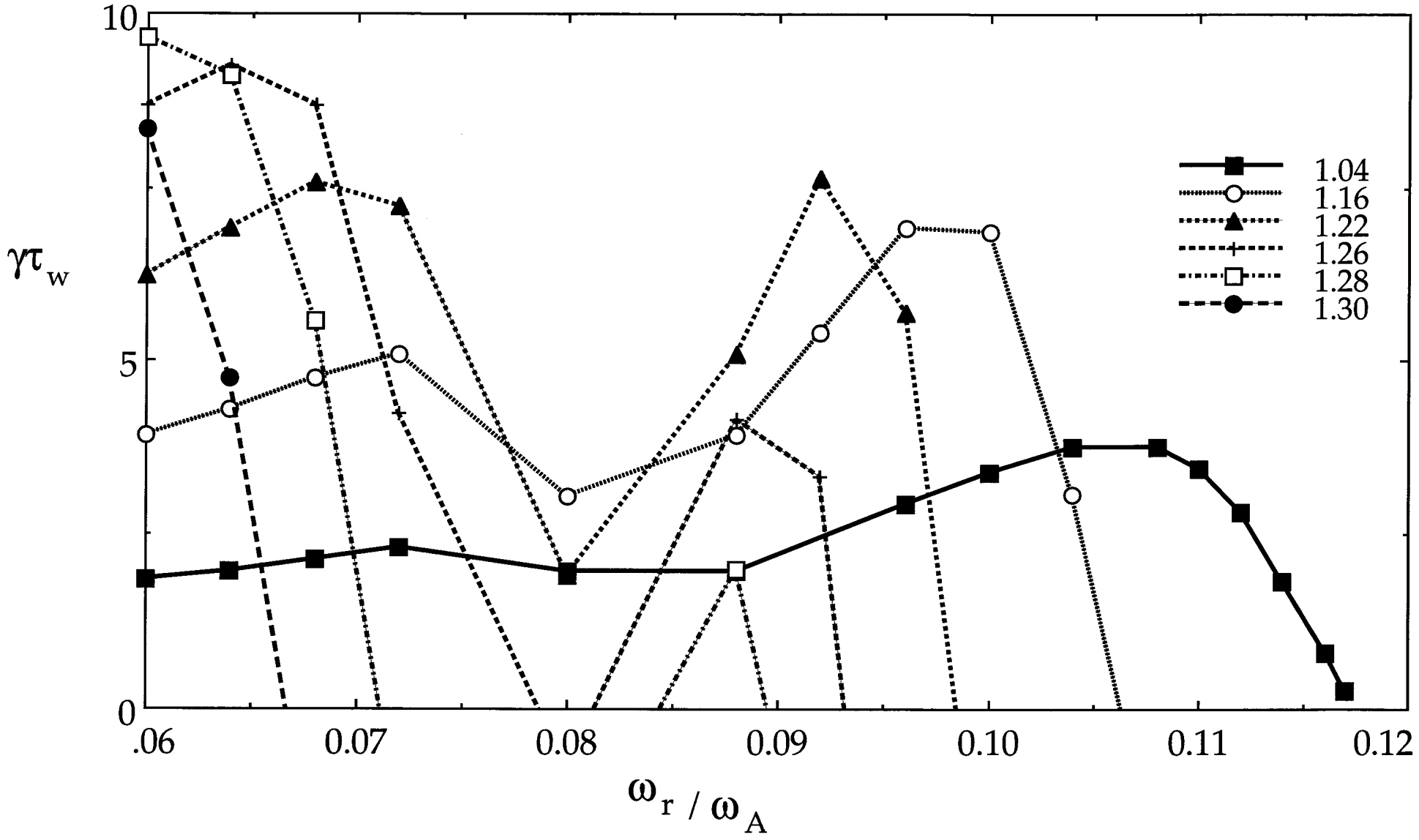
10
5
0
.06
0.07
0.08
0.09
0.10
0.11
0.12
$\gamma\tau_w$
ω_r / ω_A
1.04
1.16
1.22
1.26
1.28
1.30

Figure 15